

UDK 552.52; 620.181.4

Thermal, Ceramic and Technological Properties of Clays used in Production of Roofing Tiles – Principal Component Analysis

Milica V. Vasić¹, Lato L. Pezo², Jelena D. Zdravković^{3*}, Marija Vrebalov⁴, Zagorka Radojević¹

¹Institute for Testing of Materials IMS, Bulevar vojvode Mišića 43, 11000 Belgrade, Serbia

²University of Belgrade, Institute of General and Physical Chemistry, Studentski trg 12, 11000 Belgrade, Serbia

³Innovation Centre - Faculty of Technology and Metallurgy, University of Belgrade, Karnegijeva 4, 11000 Belgrade, Serbia

⁴a.d."Polet" IGK, Železnička 13, 23272 Novi Bečej, Serbia

Abstract:

This research describes a study of 11 selected samples of brick clays applied in roofing tile production, by using simultaneous thermal analysis. Additionally, the laboratory-sized samples were prepared and fired (850-950 °C) and technological properties were determined. Mathematical analysis was applied to sum all the experimental results and help discriminate the samples by their behavior during firing. The samples, very similar according to mineralogical and chemical content, as well as granulometry tests, were successfully grouped using principal component analysis (PCA). The PCA was used to explore and easily visualize the differences between samples. The PCA performed for differential thermal analysis (DTA), differential scanning calorimetry (DSC) and differential thermogravimetry (DTG) curves clearly showed that the heat flow was mainly influenced by carbonate content and its grain size, while DTG discriminated samples according to the contents of clay minerals and carbonates. In addition, dilatometry analysis revealed which samples underwent the highest densification during the firing process. The PCA analysis of fired products properties showed that the highest correlations were between water absorption with firing shrinkage and compressive strength.

Keywords: Brick clay; Thermal analyses; Principal component analysis, Dilatometry.

1. Introduction

At the beginning of the XIX century in Serbia, there were so-called Brick nomads. They traveled with some of equipment asking and made bricks at a site where needed. The landlord who builds a house gave a part of the field to dig the earth, as well as space for drying hand-formed products in the air and later cladding oven. The experience of the nomads to assess the appropriate type of raw material was crucial to the quality of the product. At that time, solid brick was the only type produced, and this product in Serbia has survived to this day, although it ceased to be used in the past two decades in Europe [1-4]. It is considered that today, despite technical prosperity and numerous studies in this field, we would have much to learn from the old-technology brick makers.

*) Corresponding author: jtanasijevic@tmf.bg.ac.rs

Development of the brick industry in the world starts by producing the first extruder for molding products in 1835. In Serbia, the building of brick factories (including roofing tile production) started at the end of the XIX century [1-5]. In 2010, there were about 90 brick factories, of which more than a half had primitively production. Today, a number of factories dramatically decline, while modern production must meet the growing demand for improving the quality of products and the efficacy of the production process [1-4]. Recently, a great effort has been made to improve the knowledge of such a heterogeneous material such as brick clay, and optimize production of different brick products in Serbia, by using mathematical methods [3, 4, 7-9].

In this work, differential thermal analysis (DTA), differential scanning calorimetry (DSC), thermogravimetry and dilatometry tests are done, on the example of 11 brick clay samples used in roofing tile production. The laboratory samples are extruded, carefully dried and fired at temperatures in a range between 850-950 °C. The effect of temperature was investigated in terms of independent mechanical parameters such as compressive strength (CS), water absorption (WA), firing shrinkage (FS), weight loss during firing (WLF) and volume mass of cubes (VMC).

This research was governed by an idea to reveal whether it is possible to discriminate between the brick clay samples, on the basis of qualitative analysis of differential thermal analysis (DTA), differential scanning calorimetry (DSC) and differential thermogravimetry (DTG) data, as well as the temperature dilatation data and the quality parameters of the final products subjected to various processing temperatures (ceramic and technological properties). Such an analysis was never done in this field before, the only similar idea was found in the area of food testing [10]. The obtained results were analyzed using principal component analysis (PCA) to classify and discriminate between the samples. This analysis could also be very useful as another method for authenticity control in practice.

2. Materials and Experimental Procedures

2.1. Characterization of brick clay samples and fired products

The brick clay samples were collected from sites in South Serbia, near brick factories which produce roofing tiles and ceiling elements. The sampling localities and the assigned marks of the samples were: Mala Plana (MP7, MP8, MP9, and MP10), Leskovac (LE14, LE15, LE16, LE17, and LE18), and Vlasotince (VL3 and VL4).

Simultaneous TG-DTA/DSC measurements were carried out by TA Instruments device (SDT Q600, New Castle, GB). Sample masses (≈ 20 mg) in the form of powder were heated in platinum (DTA signal) and alumina (DSC signal) crucibles, from room temperature up to 1000 °C under the air atmosphere (flow rate: 100 cm³min⁻¹; heating rate: 20 °Cmin⁻¹) [11].

Dilatometric analysis showed the behavior of dry products during firing. The tests were carried out using a Linseis dilatometer (Robbinsville, NJ, USA) with a rhodium oven and thermocouple platinum-rhodium (L76). The extruded sample was dried overnight at 105 °C and then, after cooling to room temperature, heated in the dilatometer. The temperature increment was 10 °Cmin⁻¹, and the sample was held up at the final temperature of 1000 °C for 1 h. Length changes were recorded every minute during the heating (and cooling) stage.

After collecting, the samples were dried in the oven at 105±5 °C until constant mass and then milled to obtain particles less than 1 mm. The clays were moistened by mixing with about 24–26 wt.% of tap water. They were left to rest for 24 h in sealed nylon bags to obtain homogenous moist distribution. The shaping process was done using a laboratory extruder (Händle, Germany). The laboratory samples were formed as tiles (120×50×14 mm³), hollow blocks with vertical voids (55.3×36×36 mm³) and cubes (30×30×30 mm³). After shaping, the samples were dried in the air, and later in a laboratory

dryer applying a slow regime at the beginning. Later, they were subjected to the temperature of 105 ± 5 °C, and dried to a constant mass. The firing was done in the oxygen atmosphere electric furnace, with an average heating rate of 1.4 °Cmin⁻¹ up to 610 °C, and afterward with the rate of 2.5 °Cmin⁻¹ until the final given temperature is reached, at which the samples were treated for 2 h [4, 6, 12]. The firing was conducted at 850, 870, 900, and 950 °C.

Firing shrinkage (FS) was obtained by the relative variation in length of the tiles using a caliper (± 0.01 mm precision).

Weight loss during firing (WLF) was determined by measuring the samples on a scale having 0.001 g precision and was calculated as a ratio between the weight lost during firing and the starting weight of samples. The results were expressed in weight percent (wt.%).

Compressive strength (CS) was determined using the laboratory hydraulic press Alfred Amsler, CHD, Switzerland [6, 12]. Three specimens for each combination of sample shape (blocks and cubes) and firing temperature were tested. The samples were flattened to ensure that the surfaces were parallel. CS is then tested on the single samples (without mortar usage), having the bottom area of 0.002 m² for blocks and 0.0009 m² in the case of cubes, using a loading rate of 0.6 kNs⁻¹. The results reported were the average of three specimens with a variation of no more than 10 %.

Water absorption (WA) was evaluated by soaking of the samples in water for 24 h, according to the standard SRPS EN 772-21, and later volume mass of the cubes (VMC) was calculated as weight of fired samples divided by the volume of water displaced by the sample (previously saturated with water) in the measuring cylinder [4].

2.2. Statistical analysis

Principal component analysis (PCA) has been frequently used for fingerprinting of curves and experimental data of similar samples [13, 14]. Prior to the PCA, experimental results were checked for existence of outliers. All samples were grouped in a multi-dimensional factor space and four PCA graphics were plotted, according to results presented in DTA/DSC and TGA curves, dilatometric data, and the fired brick properties. This technique was also performed to classify the brick clay samples subjected to different temperatures (850-950 °C).

PCA decomposed the original matrix into several products of multiplication, and that were loading (different samples) and score (different peaks in DTA/DSC and TGA curves, dilatometric data, or brick quality parameters) matrices. Different samples subjected to various temperatures were taken as variables (column of the input matrix) and DTA/DSC and TGA peaks, dilatometric data, or brick quality parameters as cases (rows of the matrix).

Descriptive analysis of the data and PCA were performed using the software package STATISTICA 10.0 (StatSoft Inc., Tulsa, OK, USA).

3. Results and Discussion

The qualitative presence of minerals in tested brick clays, as well as sampling locations and brick clay types, are presented in Tab. I:

Before any further discussion, it is of a great importance to bear in mind that the studied brick clay samples were very similar to each other, by means of their chemical/mineralogical composition and granulometry. Mineralogical analysis showed that the most abundant mineral in all the samples was quartz. To a lesser amount, it is followed by feldspar (plagioclase). Calcite in great amount was detected by X-ray analysis in some of the samples (LE18, MP9, and MP10). Concerning minerals from the group of layered silicates, the following were found: swelling smectite, kaolinite and mica. Chlorite was detected in low quantity in most of the samples (LE14-18 and MP10). According to granulometry analysis,

the samples contained between 20 wt.% (MP7 and MP8) and 26 wt.% (LE16) of clay fraction. Chemical analysis showed Al₂O₃ content was 15 wt.% - 20 wt.%, and Fe₂O₃ between 6 wt.% - 7 wt.%.

Tab. I Contents of minerals in brick clays.

Sample	Q	F	H	Ch	M	K	C	D	Sampling location
LE14	+	+ _l	+	+ _l	+	+	+ _l	-	Leskovac
LE15	+	+ _l	+	+ _l	+	+	+ _l	-	Leskovac
LE16	+	+ _l	+ _h	+ _l	+ _h	+ _h	-	-	Leskovac
LE17	+	+ _l	+	+ _l	+	+	+ _l	-	Leskovac
LE18	+	+ _l	+	+ _l	+	+	+ _l	-	Leskovac
MP7	+	+ _l	+ _h	-	+ _h	+ _h	+	-	Mala Plana
MP8	+	+ _l	+ _h	-	+ _h	+ _h	+	-	Mala Plana
MP9	+	+ _l	+	-	+	+	+ _h	+ _h	Mala Plana
MP10	+	+ _l	+	+ _l	+	+	+ _h	-	Mala Plana
VL3	+	+ _l	+ _l	-	+	+	-	-	Vlasotince
VL4	+	+ _l	+ _l	-	+	+	-	-	Vlasotince

Q – quartz; F – feldspat; layered silicates (H – hydromica, Ch – chlorite, M – montmorillonite, K – kaolinite), carbonates (C – calcite, D - dolomite), +_h - present in high rate, + – present, +_l – present in low rate, □ - not present

Carbonates content, determined by using a calcimetry method [2], varied between 0.0 wt.% in VL3 and VL4, and then 1.2 wt.% and 4.0 wt.% in LE samples. MP samples showed the highest variation, when carbonates content is concerned, while around 2 wt.% in MP7 and MP8, it reached nearly 8 wt.% in MP10 and 11 wt.% in MP9.

3.1. Thermal analysis

The main results of thermal analyses are summarized in Tab.s .II-IV.

Tab. II Thermogravimetric analysis results.

Sample	Stage	Temperature range	DTG peak maximum	Mass loss /Wt. %
		°C	°C	
MP7	1	30-133.5	70	3.68
	2	133.5-595	486	3.06
	3	595-1020	679.5	1.65
MP8	1	30-134.4	72.4	5.29
	2	134.5-594	159.2 475.5	4.18
	3	595-1020	684.7	2.08
MP9	1	30-127	63.4	5.39
	2	127-600	510	4.24
	3	600-1020	712	5.63
MP10	1	30-133.5	64.5 76.3	3.47
	2	133.5-552	484.3	3.42

	3	552-1020	706.3	5.18
	1	30-134.4	80.0	3.41
LE14	2	134.4-592.6	149.6 287.3	3.62
	3	592.6-1015	493.8 681.5	1.82
	1	30-148.2	90 145	1.51
LE15	2	148.2-581.4	274.1 473.7	3.30
	3	581.4-120	657.6	1.19
	1	30-133.5	38.6	4.34
LE16	2	133.5-1020	144.5 266.5	4.65
	3	594.9-1020	472.3 712.5	3.14
	1	30-133.5	73.2	3.75
LE17	2	133.5-584.9	157.1 271.5	3.01
	3	584.9-1020	484.9 712.5	3.14
	1	30-134.4	78.5	4.0
LE18	2	134-585.7	156.9 278.7	3.42
	3	585.7-1020	493.9 687.9	1.58
	1	30-114.4	66.8	2.66
VL3	2	114.4-1020	137.6 268.3	4.74
	3	585.7-1020	458.75 687.9	1.58
	1	30-115.3	69.0	3.05
VL4	2	115.3-1020	133.9 259.9	5.09
	3	585.7-1020	463.2 687.9	1.58

The thermogravimetric analysis showed that from room temperature up to 135 °C, physically adsorbed and interlayer water is released, which is manifested as an endothermic peak in corresponding DTA/DSC curves. The endothermic reaction between 100-250 °C is characteristic for the escape of interlayer water of smectite, while for illite it goes up to 300 °C. The highest content of adsorbed and interlayer water was observed in MP9 (5.39 %), MP8 (5.3 %), LE16 (4.3 %) and LE18 (4.3 %), while the least amount was found in LE15 (1.5 %) (Tab. II). Considering the values of the first DTG peak maxima for all samples, attributed to the water release, the highest values were detected for LE14 (80 °C) and LE16 (90 °C).

The water loss from hydroxides (goethite) observed as an endothermic peak in corresponding DTA/DSC curves around 250 °C proceeds to a large exothermic effect around 320 °C due to the combustion of organic matter [12]. The exothermic effect is especially pronounced for LE15-18 and VL3-4 samples. The release of hydroxyls of iron along with the combustion of organic matter is accompanied by the mass loss in TG/DTG curves, reflecting as a small DTG peak in the temperature range 250-300 °C in all samples apart for MP7-10

(Tab. II). Therefore, MP7-10 samples probably contained the lower amount of organic matter compared to others.

Small and broad endothermic peak around 485 °C in DTA/DSC curve, somewhat more pronounced for LE16 and MP8 than for others, followed by the mass loss between 300 and 550 °C, is probably due to the loss of chemically bonded water. The higher intensity of these peaks for LE16 and MP8 is related to dehydroxylation of structural OH⁻ in micas and smectite, suggesting their higher content. For MP9 this process is barely visible, indicating the lower amount of micas. In all samples, in DTA/DSC curves, a small sharp endothermic peak without associated mass loss has been observed around 573 °C, which is related to the transformation of α -quartz to β -quartz [12, 15].

The third degradation stage, associated to decarboxylation of calcite, is manifested with an especially intense endothermic reaction in corresponding DTA/DSC curves for MP9 and MP10, moderately for MP7, MP8, and barely visible in the cases of LE14 and LE17. The endothermic minimum in the DTA curve of MP9 sample, ascribed to decarboxylation of calcite, was at a higher temperature compared to the other samples probably due to the presence of dolomite [16, 17]. Very wide and small endothermic peak from 600-900 °C in DTA curves for VL3-4 and LE16 accompanied with a negligible mass loss, supporting previous findings, is related to the absence of carbonates. Small endothermic effect around 900 °C, observed in the samples without or with very low calcite content (VL3, VL4, LE14-16, and LE18), is attributed to the final destruction of the crystal lattice of smectite. This endothermic effect precedes the formation of high-temperature spinel phase [18].

According to the TG/DTG curves, the highest mass loss up to 1000 °C was obtained for MP9, MP10, MP8, and LE17, moderately for LE14, LE16, and LE18 and the lowest for VL3, VL4, and LE15, which is mostly related to carbonate contents. In the 850-1000 °C temperature range, for most of the samples, DTA/DSC curves are not accompanied by a mass loss in corresponding TG/DTG curves suggesting that all products of decomposition remain as solid phases in the sample. The only exception was the MP), which showed less than 1 % of the mass loss. This result was in agreement with other authors, which concluded that carbonates are fully transformed either into burnt lime (CaO) or into a mixture of lime and periclase (MgO) at 800 °C [16, 19]. Considering the composition of the samples, the most probable reactions were related to crystallization of new phases during heating.

Tab. III The parameters of DSC peaks in the 800-1000 °C temperature range.

Sample	Temperature interval/°C	Peak Area/Jg ⁻¹	Maximum temperature/°C
LE14	895-1000	7.40	975
LE15	874-977	9.85	925
LE16	872-979	12.0	919
LE17	877-984	7.04	919
LE18	871-1000	14.3	930
MP7	850-974	27.3	907
MP8	876-975	22.3	914
MP9	800-1000	160	886
MP10	869-957	5.5	903
VL3	916-1000	11.0	972
VL4	928-1000	8.05	968

The highest differences among the samples were noticed in the 850-1000 °C temperature range. This interval is also of a special interest, considering the influence of pre-firing of minerals on the final products. The parameters of DSC and DTA peaks at high temperatures are summarized in Tab.s III and IV. The changes of energy due to the phase transition of minerals are much smaller than that of dehydration or a decomposition reaction, which are more energy-intensive processes [20]. Considering the fact that the MP9 sample

exhibits the highest mass loss from 600-1020 °C (Tab. II), the larger area in corresponding DSC/DTA curves is therefore expected (Tab.s III and IV). Since MP9 contains dolomite in the excess of SiO₂, the most probable reaction after 900 °C is its transformation to diopside [19].

Tab. IV The parameters of DTA peaks in the 850-1000 °C temperature range.

Sample	Temperature interval/°C	Peak Area/ μ V min mg ⁻¹	Maximum temperature/°C
LE14	850-1000	0.04815	974.6
LE15	868-985	0.04616	921.4
LE16	870-971	0.05498	919.2
LE17	863-983	0.02622	919.0
LE18	870-998	0.05547	928.6
MP7	850-975	0.1280	903.2
MP8	850-973	0.1226	913.4
MP9	850-950	0.590	885.0
MP10	850-952	0.03515	901.3
VL3	916-1000	0.08299	971.9
VL4	913-1000	0.06677	967.5

The highest peak maxima were observed for LE14, VL3, and VL4 (Tab.s III and IV), due to the formation of a high-temperature phase such as mullite [21]. In the case of samples with higher calcite content (MP9 and MP10), CaO reacts with decomposed clay mineral form yielding phases like anorthite and wollastonite, rather than mullite [22]. In all the samples, the most abundant mineral was quartz. The transformation of quartz to tridymite, which occurs around 870 °C, is associated with significant volume change, which was not observed in the dilatometry diagrams suggesting the absence of it. The reason for this can be that in the presence of mineralizer such as ferric oxide, tridymite may be formed at higher temperatures [12, 17].

3.2. Principal component analysis of brick clays thermal behavior

The analysis of dissimilarities in the brick clay samples subjected to various temperatures was investigated by means of PCA. Firstly, the results of DSC analyses of observed samples were studied. The number of factors retained in the model for proper classification of the DSC data, in the original matrix was observed as loading (which presented different samples) and scores (which introduced peak area in the PCA analysis) by application of Kaiser and Rice's rule [13]. This criterion retains only principal components (PC) with Eigenvalues larger than 1. The first PC explained 98.56 % of the total variance (the first Eigenvalue equals 10.84) in the DSC data registered on the curves (temperatures between 850-950 °C) (Fig. 1). Projection of the variables on the first factorial plane indicated that all samples and the temperatures contribute mostly to the first PC, and thus to the total variability of the basic set, which is explained by general high similarities among samples. The position of the samples in the first factor plane was determined by heat flow at the chosen temperature range, with a raster of 10 °C.

PCA graphic of DSC curves showed discrimination between the samples, indicating that LE15-18, VL3, and VL4 showed the lowest heat flow values in the observed range. The fact is that the samples containing more carbonates showed greater changes in heat flow. The changes of energy due to the phase transition of minerals are much lower than that of dehydration or a decomposition reaction [20]. The only sample whose position on the PCA diagram could not be explained by carbonate content was LE14. Namely, it consisted of the coarsest carbonate grains among all (lime pop-corns showed in the fired samples), and thus

the highest energy (heat flow) was needed in order to break them down. Since it was previously concluded (TGA curves) that there practically was no mass loss in the studied temperature period, the rest of carbonates which are not decomposed reacted with clay minerals and formed calcium silicates [12]. The process can start at temperatures higher than 800 °C, at the same period when the most significant textural and mineralogical changes are expected in the samples containing carbonates. Gehlenite starts to form by reaction between CaO, Al₂O₃, and SiO₂ at grain boundaries. Wollastonite is formed from quartz and CaO [19, 23]. In the case of samples MP7-9, wide exothermic peaks are found between 850 and 930 °C, probably due to the onset of clay sintering and change in crystalline structure [24]. The effect was the most pronounced in MP9.

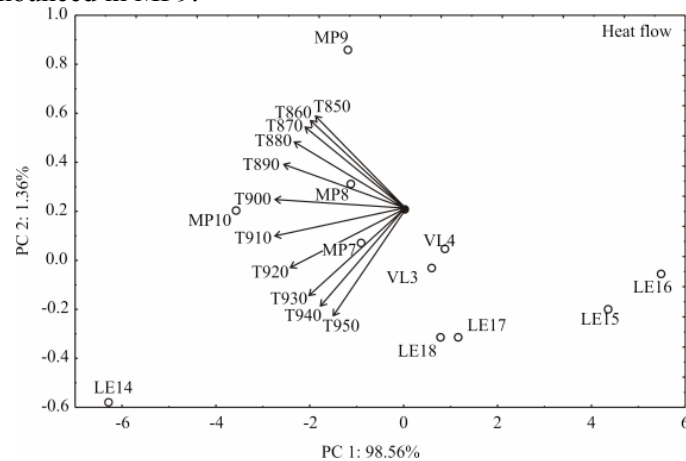


Fig. 1. Projection of variables on the first factor plane, based on DSC curves of brick clay samples (temperatures between 850-950 °C).

The increased heat flow analyzed in the temperature range (850 - 930 °C) is observed in the case of samples MP7-10, while the maximum heat flow is determined for the sample LE14 between 920-950 °C, possibly due to complete illite breakdown [16, 19].

The DTG data were also studied using the PCA analysis. The first PC explained 65.40% of the total variance (the first Eigenvalue equals 7.19) in the DTG data registered on the curves (temperatures between 850-950 °C) (Fig. 2):

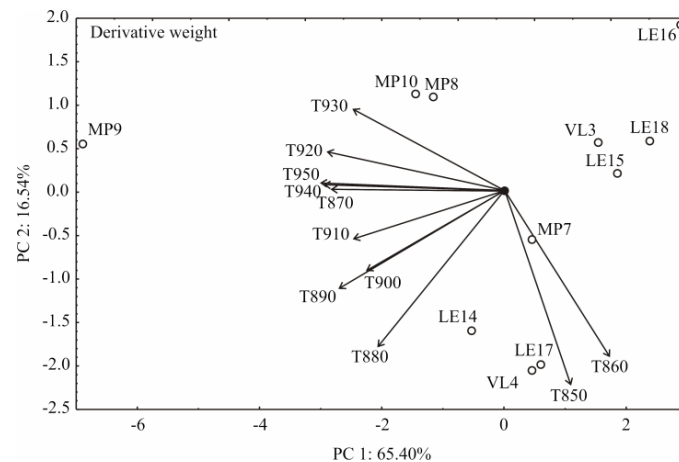


Fig. 2: Projection of variables on the first factor plane, based on DTG data of brick clay samples (temperatures between 850-950 °C).

The minimal changes in weight were observed for the samples LE15, LE16, LE18, and VL3, which was in accordance with weight loss during firing (WLFT, WLFB and WLFC) (Paragraph 3.3.). Bigger changes in weight were observed for samples MP7, MP8, MP10, LE14, LE17, and VL4 (around 0.1 wt.%). The maximal derivative weight was observed in the case of sample MP9 between 920 and 950 °C (0.4 wt.%). The process could be regarded to the final breakdown of the clay mineral lattice and the loss of a small amount of water which results from the loss of the last hydroxyls [11, 25].

The extreme cases (minimal and maximal weight changes in the LE16 and MP9, respectively) found by PCA (Fig. 2), were presented in Fig. 3 to show the convenience of such an analysis, which easily marked the differences. The reason for these differences was in the contents of carbonates and clay minerals.

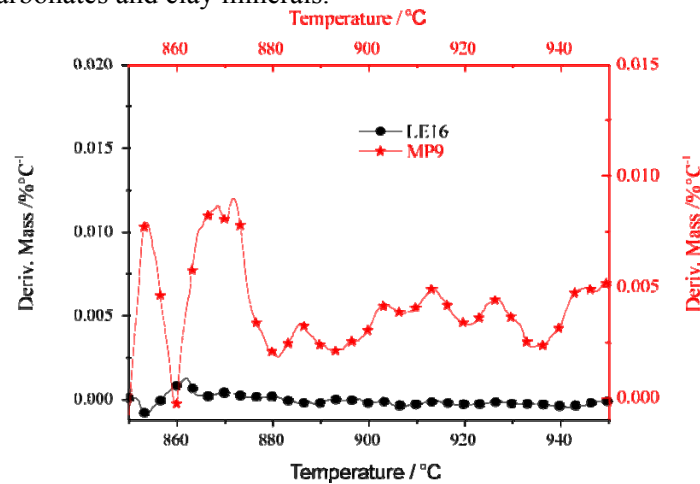


Fig. 3. DTG in the 850-950 °C range for extreme samples found by PCA.

Thermal dilatation of observed samples was also studied using PCA analysis. The first PC explained 93.34 % of the total variance (the first Eigenvalue equals 10.27) in the thermal dilatation data registered (temperatures between 850-950 °C, raster 10 °C) (Fig. 4). Projection of the variables on the factorial plane indicated that all samples and the temperatures contributed mostly to the first PC, and thus to the total variability of the basic set. This means that all the tested samples showed pretty similar behavior while testing thermal dilatation.

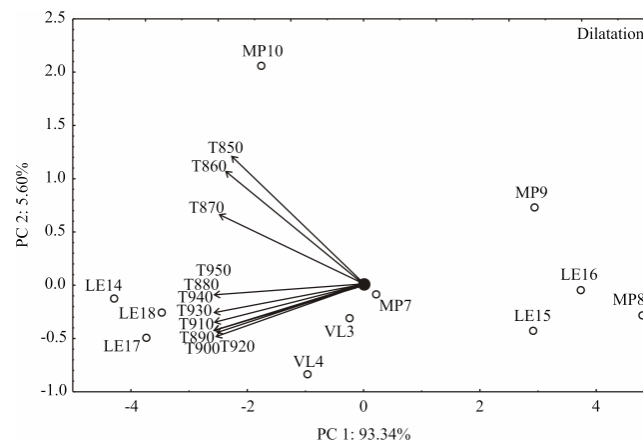


Fig. 4. Projection of variables on the first factor plane, based on thermal dilatation data of brick clay samples fired at 850-950 °C.

All dilatometric curves showed a plateau between 600 and 850 °C, typical for illitic clays [26]. In the selected temperature range (850-950 °C), all the samples showed fast shrinkage with the temperature increase, which can lead to the conclusion that this was the exact range where sintering was taking place [27-29]. Concerning dilatometric curves, verification (accompanied by partial melting) commenced at 840-860 °C for all the samples. The melting process was not recorded in DTA/DSC curves since this endothermic thermal effect has a low intensity [20]. MP8-9 and LE15-16 showed the highest shrinkage, while LE14, LE17 and LE18 showed the lowest. Milder dilatations were observed for samples VL3-4, MP7 and MP10. It may be concluded that LE14, LE17, and LE18 underwent the highest densification through agglomeration of the fine clay particles, in the 880-940 °C range.

It is worth to mention that dilatometric curves, beyond the observed range, intensively in sample MP9, and less pronounced in MP10, showed "U" shape, with maximum peaks about 960 °C. This phenomenon is not viewed as having much significance in the literature, according to the findings of the present study. It is visible on some of the diagrams, and the authors showed that the increased carbonate content induces greater shrinkage/expansion maximums after 900 °C, where these samples are considered susceptible to cracking [30]. The effect is explained by the expansive formation of anorthite in samples rich in carbonates [19, 31].

3.3. Ceramic and technological properties of brick samples

Results of ceramic and technological properties are reported in Tab. V. In here presented cases, it is again showed that fired samples properties did not change according to a linear law against temperature [3]. It can be seen that MP9 and MP10 showed extreme WLF values, while VL3 and VL4 underwent the lowest weight losses, which was in accordance with the contents of carbonates. It is hard to distinguish between so many results in the Tab., so PCA was done and discussed later on.

Tab. V Properties of laboratory brick products at different firing temperatures.

No.	Site	T /°C	FS /%	WLFT /%	WLFB /%	WLFC /%	CSB /MPa	CSC /MPa	WAT /%	WAB /%	WAC /%	VMC /gcm ⁻³
1	LE14	850	-0.17	6.45	5.90	6.33	29.06	65.84	11.11	11.48	12.08	1.90
2	LE14	870	0.01	6.52	5.99	6.22	31.70	66.82	10.60	10.99	11.22	1.95
3	LE14	900	0.19	6.58	6.07	6.12	34.34	67.79	10.08	10.51	10.35	2.01
4	LE14	950	0.48	6.50	6.08	6.07	14.27	30.97	10.09	10.87	10.25	1.92
5	LE15	850	0.63	6.03	6.48	6.40	24.77	61.54	9.76	9.64	9.74	2.03
6	LE15	870	1.01	6.07	6.58	6.46	23.14	68.91	8.90	8.15	8.87	2.03
7	LE15	900	0.25	6.00	6.39	6.34	26.41	54.18	10.61	11.12	10.62	2.03
8	LE15	950	0.72	6.10	6.63	6.46	25.01	66.25	10.10	9.48	9.46	2.03
9	LE16	850	0.67	6.22	6.19	6.08	26.59	49.47	9.02	9.20	9.54	1.94
10	LE16	870	1.17	6.34	6.30	6.21	28.31	39.24	7.77	8.31	8.45	1.99
11	LE16	900	0.17	6.10	6.08	5.96	24.88	59.69	10.27	10.10	10.62	1.88
12	LE16	950	0.59	6.20	6.36	6.17	24.23	69.37	9.70	9.72	10.03	1.99
13	LE17	850	0.30	6.49	6.35	6.40	19.08	61.62	10.60	10.13	11.18	1.97
14	LE17	870	0.51	6.60	6.44	6.54	21.24	58.86	9.88	9.48	10.60	1.87
15	LE17	900	0.09	6.37	6.26	6.25	16.92	64.38	11.32	10.77	11.75	2.06
16	LE17	950	0.28	6.44	6.27	6.29	17.52	62.26	10.74	10.12	11.05	2.06
17	LE18	850	0.60	6.97	7.00	6.89	26.41	63.94	8.99	8.35	9.16	1.99
18	LE18	870	0.87	7.04	7.00	6.97	23.95	60.80	8.24	7.63	8.48	1.95

19	LE18	900	0.33	6.91	7.00	6.80	28.87	67.08	9.74	9.06	9.84	2.03
20	LE18	950	0.57	6.94	7.04	6.83	22.07	67.15	8.81	8.09	9.42	2.04
21	MP7	850	0.21	6.72	6.27	6.59	34.98	55.83	8.00	9.40	8.98	1.98
22	MP7	870	0.38	6.79	6.36	6.59	34.81	58.78	8.26	8.88	8.83	1.94
23	MP7	900	0.56	6.87	6.45	6.59	34.65	61.74	8.52	8.35	8.69	1.90
24	MP7	950	0.48	6.94	6.83	6.93	40.80	105.93	7.75	7.50	7.62	1.97
25	MP8	850	0.42	7.19	6.77	7.14	37.69	85.68	8.05	8.73	8.09	1.88
26	MP8	870	0.66	7.43	7.00	7.32	37.16	80.88	8.13	8.00	7.54	1.99
27	MP8	900	0.89	7.66	7.23	7.50	36.64	76.07	8.22	7.26	6.99	2.10
28	MP8	950	1.45	7.58	7.33	7.55	86.86	122.80	6.55	5.95	5.64	2.09
29	MP9	850	-0.15	8.70	8.69	8.81	38.54	75.00	10.38	10.94	10.31	1.84
30	MP9	870	-0.10	8.91	8.71	8.85	36.49	86.80	11.16	10.56	10.42	1.84
31	MP9	900	-0.05	9.12	8.72	8.89	34.45	98.59	11.93	10.18	10.52	1.84
32	MP9	950	-0.14	9.23	9.07	9.27	40.36	102.52	11.71	10.21	10.45	1.88
33	MP10	850	-0.38	9.99	9.52	9.74	18.02	56.07	10.39	10.08	10.24	1.81
34	MP10	870	-0.41	9.62	9.29	9.37	19.84	52.61	10.86	9.97	10.46	1.81
35	MP10	900	-0.44	9.25	9.07	9.00	21.67	49.15	11.32	9.85	10.67	1.81
36	MP10	950	-0.52	9.39	9.31	9.21	20.64	73.05	12.10	9.80	10.63	1.81
37	VL3	850	0.16	4.78	4.87	4.84	29.47	66.82	10.42	10.01	10.05	1.92
38	VL3	870	0.11	4.76	4.85	4.80	28.88	64.20	10.62	10.17	10.41	1.92
39	VL3	900	0.20	4.80	4.89	4.87	30.06	69.44	10.22	9.85	9.68	1.92
40	VL3	950	0.59	4.92	4.96	4.83	30.24	68.91	9.25	9.03	9.13	1.91
41	VL4	850	0.13	5.84	6.22	6.18	24.85	48.16	10.97	10.93	11.25	2.00
42	VL4	870	0.10	5.77	6.07	6.13	23.05	52.10	11.14	10.96	11.35	2.08
43	VL4	900	0.15	5.91	6.36	6.23	26.65	44.22	10.80	10.89	11.14	1.93
44	VL4	950	0.42	5.98	6.24	6.39	25.69	57.58	10.17	9.88	9.94	2.07

The final laboratory bricks quality was observed according to ceramic and technological characteristics, such as CSB, CSC, WAB, WAC, WAT, FS, WLFB, WLFC, WLFT, and VMC, in the PCA analysis (Fig. 5). The dots No. 1 - 44 are the cases presented in Tab. V.

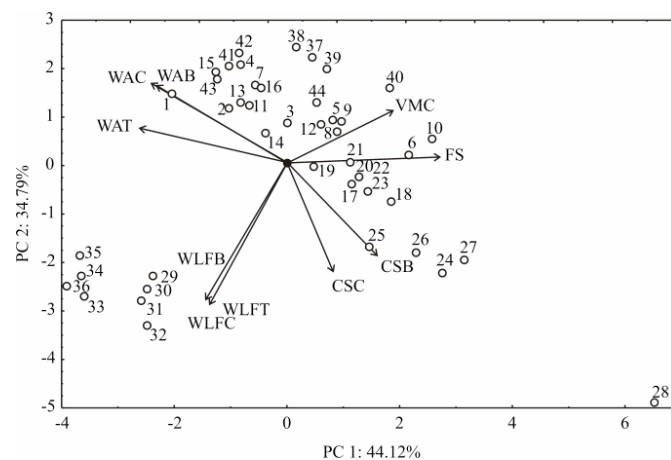


Fig. 5. Projection of variables on the first factor plane, based on ceramic and technological characteristics of bricks fired at 850-950 °C.

Correlation analysis of the observed properties could be perceived from Fig. 5. The strongest negative correlation was found between FS and WA, statistically significant at $p < 0.01$ level, for observed fired brick clay samples. Slightly lower, but still statistically significant negative correlation ($p < 0.01$ level) was noticed between CS and WA parameters, which is in accordance with previous results [1-4].

The first PC explained 44.12 % of the total variance (the first Eigenvalue equals 4.43) in the data registered (temperatures between 850-950 °C) (Fig. 4). The second PC explained 34.79 % of the total variance (Eigenvalue equals 3.50).

The maximum WLF values were observed for MP10 (samples 33-36) and MP9 (samples 29-32). The maximum CS values were observed for MP8 (samples 25-28) and the maximum WA values were observed for VL4 (samples 41-43). On the first place, the results depended on clay mineral contents, together with carbonate contents and their grain sizes. Higher content of clay minerals improves CS, as well as newly formed calcium-silicates. On the other hand, unreacted carbonates burn and leave pores behind, which weakens the products, and gives higher WA values [12].

4. Conclusion

Comparison of the samples using multivariate statistical techniques showed to be very effective for the discrimination purposes in this research. Principal component analysis was used to show sets of experimental results concerning thermal, ceramic and technological analysis and present the differences between the samples in the 850-950 °C range. This research revealed and confirmed that the heat flow depended on calcite content and its' grain size, that mass loss was mostly influenced by the combined effect of clay minerals and calcite content, and that fine clay particles quantities influenced higher densification.

The comparison of sample properties after firing at different temperatures is rather difficult, especially when the explored characteristics of the samples are very similar to each other. For that purpose, multivariate PCA analysis turned out to be very convenient tool for discriminating and visualizing of the observed differences. In addition, the presented method in which PCA is used for the exploratory purposes saves the time needed for the analysis of many properties concerning various samples. Hence, the presented analysis may have great potential as another method for authenticity control in practice.

Acknowledgments

Support for this work by the Ministry of Education, Science and Technological Development of the Republic of Serbia (Grants No. III45008, TR31055 and III45007) is gratefully acknowledged.

5. References

1. M. Arsenović, Optimization and prediction of the quality of materials, process and final properties of heavy clay products by mathematical modeling of the characteristic parameters, PhD dissertation, Faculty of Technology and Metallurgy, Belgrade University, Belgrade, 2013.
2. M. Arsenović, L. Pezo, Z. Radojević, S. Stanković, Hem. Ind. 67 (2013) 811.

3. M. Arsenović, L. Pezo, S. Stanković, Ž. Lalić, Z. Radojević, Ceram. Int. 39 (2013) 6277.
4. M. Arsenović, S. Stanković, L. Pezo, L. Mančić, Z. Radojević, Ceram. Int. 39 (2013) 3065.
5. A. T. Green, C. H. Stewart, Ceramics, a symposium arranged and edited by Green and Stewart. British Ceramic Society 1953, Stoke-on-Trent pp. 755.
6. M. Arsenović, Z. Radojević, S. Stanković, Ž. Lalić, L. Pezo, Ceram. Int. 39 (2013) 1667.
7. M. Arsenović, L. Pezo, S. Stanković, Z. Radojević, Appl. Clay Sci. 115 (2015) 108.
8. Z. Bačkalić, J. Ranogajec, R. Marinkovic-Neducin, M. Vrebalov, M. Radeka, J. Eur. Ceram. Soc. 27 (2007) 1865.
9. L. Sidjanin, J. Ranogajec, D. Rajnovic, E. Molnar, Mater. Design 28 (2007) 941.
10. J. Petrović, N. Perišić, J. Dragišić-Maksimović, V. Maksimović, M. Kragović, M. Stojanović, M. Laušević, M. Mihajlović, J. Anal. Appl. Pyrolysis 118 (2016) 267.
11. M. Pansu, J. Gautheryou, Handbook of soil analysis: mineralogical, organic and inorganic methods. Berlin/Heidelberg/New York: Springer Verlag, 2003.
12. M. Arsenović, L. Pezo, Z. Radojević, Process. Appl. Ceram. 6 (2012) 209.
13. H. Abdi, L.J. Williams, Wiley Interdiscip. Rev. Comput. Stat. 2(2010) 433.
14. D. Radulović, A. Terzić, L. Pezo, Lj. Andrić, I. Grigorova, Sci. Sinter. 49 (2017) 247.
15. N. N. Greenwood, A. Earnshaw, Chemistry of the elements. Oxford: Pergamon, 1984.
16. R. E. Grim, R. A. Rowland, J. Am. Ceram. Soc. 27 (1944) 65.
17. R. C. MacKenzie, Differential Thermal Analysis: Fundamental Aspects, 1st ed. London: Academic Pr, 1970.
18. H. E. Gaudette, J. L. Eades, R. E. Grim, Clays and Clay Minerals 13 (1964) 33.
19. G. Cultrone, C. Rodriguez-Navarro, E. Sebastian, O. Cazalla, M. Jose de la Torre, Eur. J. Mineral. 13 (2001) 621
20. M. Földvári, Handbook of thermogravimetric system of minerals and its use in geological practice. 1st ed. Budapest: Geological Institute of Hungary, (2011) 44.
21. M. E. Ouahabi, L. Daoudi, F. Hatert, N. Fagel, Clay. Clay Miner. 63 (2015) 404.
22. M. J. Trindade, M. I. Dias, J. Coroado, F. Rocha, Appl. Clay Sci. 42 (2009) 345.
23. N. Obradović, S. Filipović, J. Rusmirović, G. Postole, A. Marinković, D. Radić, V. Rakić, V. Pavlović, A. Auroux, Sci. Sinter. 49 (2017) 235.
24. J. D. S. Favero, J. Parisotto-Peterle, V. Weiss-Angeli, R. N. Brandalise, L. B. Gomes, C. P. Bergmann, V. dos Santos, Appl. Clay Sci. 124 – 125 (2016) 252.
25. R. A. Rowland, Bulletin 169 (1955) 151.
26. G. Cizeron, Ceram. Ind. 795 (1985) 405.
27. W. D. Kingery, J. Appl. Phys. 30 (1959) 301.
28. D. Mckinney, Kinetic and finite element modeling for firing brick, All Theses 2010, Paper 761.
29. P. M. Velasco, M. P. M. Ortiz, M. A. M. Giró, D. M. Melia, J. H. Rehbein, Appl. Clay Sci. 107 (2015) 156.
30. K. E. Atcholi, E. Padayodi, J. C. Sagot, T. Beda, O. Samah, J. Vantomme, Constr. Build. Mater. 27 (2012) 141.
31. A. M. Segadães, M. A. Carvalho, W. Acchar, Appl. Clay Sci. 30 (2005) 42.

Садржај: Ово истраживање описује 11 одабраних узорака опекарских сировина коришћених у производњи црепова од глине помоћу симултане термичке анализе. Поред тога, припремљени су лабораторијски узорци који су печени на 850-950 °C, а затим су одређиване њихове технолошке карактеристике. Математичка анализа

примењена је у циљу сагледавања експерименталних резултата и бољег раздвајања узорака на основу разлика у њиховом понашању током печења. Узорци који су врло слични према минералошком и хемијском саставу, као и гранулометријској анализи, су успешно груписани применом анализе главних компоненти. Анализа главних компоненти коришћена је ради лакшег визуелног сагледавања разлика између узорака. Примена анализе главних компоненти на DTA, DSC и DTG криве јасно је показала да топлотни проток је у највећој мери условљен садржајем карбоната као и величином карбонатних зрна, док је анализа DTG кривих показала разлику између узорака према садржајима глине и карбоната. Поред тога, дилатометријска анализа је показала који су узорци претрпели највећу дензификацију током печења. Анализа главних компоненти најважнијих особина печених производа показала је највеће корелације у случају апсорпције воде са скупљањем при печењу и чврстоћом при притиску.

Кључне речи: опекарска сировина, термичка анализа, анализа главних компоненти, дилатометрија.

© 2018 Authors. Published by the International Institute for the Science of Sintering. This article is an open access article distributed under the terms and conditions of the Creative Commons — Attribution 4.0 International license (<https://creativecommons.org/licenses/by/4.0/>).

